MATHEMATICS OF COMPUTATION
VOLUME 46, NUMBER 173
JANUARY 1986, PAGES 151-169

Julia Sets and Mandelbrot-Like Sets Associated With Higher Order Schröder Rational Iteration Functions: A Computer Assisted Study

By Edward R. Vrscay

Abstract. Schröder iteration functions $S_m(z)$, a generalization of Newton's method (for which $m = 2$), are constructed so that the sequence $z_{n+1} = S_m(z_n)$ converges locally to a root z^* of $g(z) = 0$ as $O(|z_n - z^*|^m)$. For $g(z)$ a polynomial, this involves the iteration of rational functions over the complex Riemann sphere, which is described by the classical theory of Julia and Fatou and subsequent developments. The Julia sets for the $S_m(z)$, as applied to the simple cases $g_n(z) = z^n - 1$, are examined for increasing m with the help of microcomputer plots. The possible types of behavior of z_n iteration sequences are catalogued by examining the orbits of free critical points of the $S_m(z)$, as applied to a one-parameter family of cubic polynomials.

1. Introduction. The theory of iteration of rational functions, originating in the classical research of Julia [19] and Fatou [13], has witnessed a dramatic resurgence of interest in the last twenty years. The works of Brolin [6], Guckenheimer [15] and Myrberg [22] foreshadowed this revival, which has since witnessed many significant contributions: the theoretical works of Douady and Hubbard [10], [11], Mañé et al. [21], Sullivan [26] and Thurston [27], to name but a few, as well as the pioneering experimental work of Mandelbrot [20]. A comprehensive account of this research is given in the excellent review of Blanchard [5]. The fact that the iteration of even simple quadratic maps of the form $f(z) = z^2 - \lambda$ is associated with a wealth of remarkable phenomena, including Julia sets and Mandelbrot bifurcation diagrams, attests to the richness of this subject. It has understandingly become an object of vigorous pursuit in mathematical physics in the context of renormalization theory, dynamical systems and chaotic phenomena. We mention here two recent applications of Julia set theory in physics. The self-similar spectra associated with hamiltonians over fractal lattices, as discovered by Domany et al. [9], have been shown to be condensed Julia sets of a simple quadratic map by Barnsley et al. [3], with spectral densities given by the associated balanced measures. The concept of iterated electrical networks associated with the iteration of rational impedance functions has also been introduced recently [4], again finding a natural expression in the language of Julia sets of rational maps over the complex sphere.

Julia-Fatou theory and its subsequent developments are also of paramount importance in the context of numerical analysis. Here, studies have only begun [8], [17], [25]. Consider, for example, the classical Newton iteration function constructed

Received January 15, 1985.
1980 *Mathematics Subject Classification*. Primary 30D05, 30-04, 65E05.

0025-5718/86 $1.00 + $.25 per page

to converge to the zeros of a polynomial $g(z)$:

$$N(z) = z - g(z)/g'(z). \tag{1.1}$$

Clearly, $N(z)$ is a rational function. One is interested in the initial conditions for which the iteration sequence

$$z_{n+1} = z_n - g(z_n)/g'(z_n) \tag{1.2}$$

converges to a solution z^* of $g(z) = 0$. More generally, what is the set $W(z^*)$ of all initial values $z_0 \in \mathbf{C}$ for which the sequence $\{z_n\}$ converges to a given root z^*? For what $z_0 \in \mathbf{C}$ will the sequence *not* converge at all? Is it possible that the z_n converge to points or cycles other than the desired roots z_i^*? Classical theory of iteration of analytic functions [7], concerned with the behavior of sequences in the neighborhood of a fixed point p, is not equipped to attack such global problems. It is here where the Julia-Fatou theory provides insight into the dynamics of iteration schemes. For example, Curry et al. [8], with a series of numerical experiments and the main concepts of this theory, were able to catalogue the behavior patterns associated with Newton's method as applied to a one-parameter family of cubic polynomials.

A portion of this paper was motivated by [8] and could be considered an extension of it. We consider a generalized family of Schröder iteration functions [24], [16], having the form

$$S_m(z) = z + \sum_{n=1}^{m-1} c_n(z)[-g(z)]^n, \qquad m \geq 2, \tag{1.3}$$

and constructed so that the iteration sequence $z_{n+1} = S(z_n)$ converges locally to a root z^* of $g(z) = 0$ as $O(|z_n - z^*|^m)$. The function $S_2(z)$ is identical to the Newton function in Eq. (1.1). When $g(z)$ is a polynomial, the degree of the rational function $S_m(z)$ increases with m. The attractive basins of the roots z_i^*, when plotted by computer, are seen to exhibit more complicated patterns as m increases. The various types of behavior of iteration sequences $\{z_n\}$ for Newton's method are also observed in the cases $m > 2$. These higher-degree rational functions, however, possess extra fixed points which are generally distinct from the desired roots z_i^* and, if attractive, may trap an iteration sequence.

In Section 2, we explicitly introduce the family $S_m(z)$ of Schröder iteration functions, motivated by the concept of order of convergence to an attractive fixed point. The features of Julia-Fatou theory relevant to this study are then outlined. In Section 3, with the aid of microcomputer-generated plots, we examine the basins of attraction of the Schröder scheme as applied to the set of functions $g_n(z) = z^n - 1$ and compare their features with those of Newton's method. The common boundaries of these basins of attraction constitute the Julia sets of the $S_m(z)$. In Section 4, again with the aid of microcomputer plots, we examine the dynamics of Schröder maps for the one-parameter family of cubic polynomials $g_A(z)$ studied in [8]. As in Newton's iterative scheme, there exist regions M_m in complex parameter space where the critical points of the $S_m(z)$ are attracted to points or cycles which do not correspond to roots of the polynomials. These regions exhibit the morphology and classical characteristics of Mandelbrot sets. Sequences of period-doubling bifurcations are located numerically. In Section 5, we examine the effect of these Mandelbrot regions

on the attractive basin-Julia set maps in complex coordinate space. If $A \in M_m$, attractive basins for pathological cycles which do not correspond to roots of the $g_A(z)$ appear in these maps.

2. Schröder Iteration Functions and Julia-Fatou Theory. Let $f(z)$ be a complex-valued function, analytic on a suitably defined compact subset T of the complex plane $\mathbf{C}$, and having fixed point $p \in T$, so that $p = f(p)$. The fixed point p is *attractive*, *indifferent*, *or repulsive* depending on whether $|f'(p)|$ is less than, equal to or greater than one. If $f'(p) = 0$, p is termed *superattractive*. Given a starting value $z_0 \in T$, we define the iteration sequence $\{z_n\}_0^\infty$ by $z_{n+1} = f(z_n)$, $n = 0, 1, 2, \ldots$. Now assume that p is attractive, i.e., that $z_n \to p$ as $n \to \infty$. The *speed of convergence* of the iteration procedure is defined as follows. Let $e_n = z_n - p$ be the error associated with the nth iterate. Using Taylor's expansion of $f(z)$, we have

$$e_{n+1} = z_{n+1} - p = f(e_n + p) - f(p) = \frac{1}{m!} f^{(m)}(p)(e_n)^m + o\left[(e_n)^m\right], \qquad n \to \infty, \tag{2.1}$$

where m is the smallest integer for which $f^{(m)}(p) \neq 0$ (usually $m = 1$). Then $f(z)$ is said to be an *iteration function of order m*.

We now consider the construction of iteration functions of prescribed order to determine the simple roots of $g(z) = 0$. The first interesting case, $m = 2$, corresponds to quadratic convergence and yields the familiar Newton method. The point z^* is a zero of $g(z)$ if and only if it is a fixed point of $f(z) = z - h(z)g(z)$, where $h(z)$ is an arbitrary nonzero function, analytic in T. The problem is to construct $f(z)$ such that $f'(z^*) = 0$. Since

$$f'(z) = 1 - h'(z)g(z) - h(z)g'(z)$$

and $g(z^*) = 0$, we may choose $h(z) = [g'(z)]^{-1}$ to give Eq. (1.1) for $g'(z) \neq 0$.

Higher-order iteration functions may be constructed in the same spirit. If $g(z)$ is analytic in some region T, then for h arbitrarily small,

$$g(z + h) = g(z) + \sum_{n=1}^{\infty} b_n(z)h^n = g(z) + B(z) \tag{2.2}$$

where $b_n(z) = g^{(n)}(z)/n!$, $n = 1, 2, 3, \ldots$. $B(z)$ may be considered a formal power series in the variable h, whose coefficients are dependent upon the parameter z. If $b_1(z) = g'(z) \neq 0$, $B(z)$ may be formally inverted,

$$B^{-1}(z) = \sum_{n=1}^{\infty} c_n(z)h^n, \tag{2.3}$$

where [24]

$$c_n(z) = \frac{1}{n!}\left[\frac{1}{g'(z)}\frac{d}{dz}\right]^{n-1}\frac{1}{g'(z)}. \tag{2.4}$$

The coefficients $c_n(z)$ are analytic functions for $g'(z) \neq 0$, since they are also expressible in terms of powers of the $b_n(z)$ and $[b_1(z)]^{-1}$, both of which are analytic.

We now define the *Schröder iteration functions* as

$$S_m(z) = z + \sum_{n=1}^{m-1} c_n(z)[-g(z)]^n, \qquad m = 2, 3, 4, \ldots. \tag{2.5}$$

The iteration sequences defined by the $S_m(z)$ converge locally to the roots z_i^* of $g(z) = 0$ as $O[|z_n - z_i^*|^m]$. This follows from the following theorem.

THEOREM 2.1. *Let $g(z)$ be analytic for $z \in T$ and $g'(z) \neq 0$. The functions $S_m(z)$ are analytic. For every $z^* \in T$ such that $g(z^*) = 0$,*

$$S_m(z^*) = z^*, \qquad S_m'(z^*) = S_m''(z^*) = \cdots = S_m^{(m-1)}(z^*) = 0. \tag{2.6}$$

Thus, z^* is a superattractive fixed point.

Proof. See Henrici [16, p. 530].

The $S_m(z)$ functions were introduced by Schröder [24] in 1870 (see also [18]) as one of several methods to determine roots of equations. The $S_m(z)$ are truncations of a general infinite series in $g(z)$, the first three terms of which are given below:

$$\begin{aligned} S(z) = z &- \frac{1}{g'(z)} g(z) - \frac{g''(z)}{2[g'(z)]^3}[g(z)]^2 \\ &- \frac{\frac{1}{2}[g''(z)]^2 - \frac{1}{6}g'(z)g'''(z)}{[g'(z)]^5}[g(z)]^3 \cdots . \end{aligned} \tag{2.7}$$

It is easily seen that the construction of $S_m(z)$ requires a knowledge of the first $m - 1$ derivatives of $g(z)$.

From Eqs. (2.5) or (2.7), we see that for only $m = 2$—the Newton method—does the fixed point condition $S_m(z) = z$ necessarily imply that $g(z) = 0$. For $m > 2$, it implies that either (i) $g(z) = 0$ or (ii):

$$T_m(z) = \sum_{n=0}^{m-2} c_{n+1}(z)[-g(z)]^n = 0. \tag{2.8}$$

The introduction of these extra fixed points may complicate the root-finding procedure: as repulsive or indifferent fixed points they alter the basins of attraction for the roots; as attractive fixed points they may conceivably trap an iteration sequence.

Here we mention that Smyth [25] performed a detailed study of rational iteration functions constructed with a specific number M of parameters to converge to a given number n of distinct complex points with a specified order σ. For the case $\sigma = 2$ and deg(numerator) = deg(denominator) + 1, the Newton iteration functions are obtained. The Schröder functions are shown to be a subclass of a much more general group of iteration functions for $\sigma \geqslant 2$. In addition, some examples of Newton iteration functions having attractive cycles other than the desired roots of a polynomial are given.

For $g(z)$ in Eq. (2.5) a polynomial, the $S_m(z)$ are rational functions. The standard iteration theory of analytic functions is insufficient to describe the global dynamics of the Schröder method. It is here where Julia-Fatou theory can describe the possible types of behavior of iteration sequences $\{z_n\}$ associated with the $S_m(z)$. The major features are outlined below. The reader is referred to [6] for a more detailed presentation of this subject.

Let $R(z)$ be a rational function, $R(z) = P(z)/Q(z)$ where $P(z)$ and $Q(z)$ are polynomials with complex coefficients and no common factors, and $d = \deg(R) \equiv \max\{\deg(P), \deg(Q)\} \geqslant 2$. The sequence of iterates $\{R^n(z)\}$ of $R(z)$ is defined by

$$R^0(z) = z, \quad R^1(z) = R(z), \quad R^{n+1}(z) = R(R^n(z)), \qquad n = 0, 1, 2, \ldots.$$

The inverses of $R(z)$ shall be denoted by $R_i^{-1}(z)$, where the subscript index $i = 1, 2, \ldots, d$ enumerates all branches of the inverse. We now consider R: $\overline{\mathbf{C}} \to \overline{\mathbf{C}}$ where $\overline{\mathbf{C}} = \mathbf{C} \cup \{\infty\}$ denotes the Riemann sphere with suitably defined spherical metric. Given a point $z_0 \in \overline{\mathbf{C}}$, the iteration sequence $\{z_n\}_0^\infty$, given by

$$z_{n+1} = R(z_n) = R^{n+1}(z_0),$$

defines the *forward orbit* of z_0.

If $R^k(p) = p$ and $R^m(p) \neq p$ for $m < k$, then p is a *fixed point of order k*. The set of distinct points $\{p_i, i = 1, 2, 3, \ldots, k\}$, where

$$p_1 = R(p), \qquad p_2 = R(p_1), \ldots, p_k = R(p_{k-1}),$$

is termed a k-cycle. If $k = 1$, p is simply called a fixed point of $R(z)$. The k-cycle is *attractive*, *indifferent*, *or repulsive*, depending on whether the multiplier $|[R^k(p_i)]'|$ is less than, equal to or greater than one, respectively.

The Julia set $J(R)$ of the rational map R: $\overline{\mathbf{C}} \to \overline{\mathbf{C}}$ is formally defined as the set of $z \in \overline{\mathbf{C}}$ for which the family of maps $R^n(z)$ is not normal, in the sense of Montel [1]. A more working description is that $J(R)$ is the closure of all repulsive k-cycles of $R(z)$, $k = 1, 2, 3, \ldots$. Its complement, $F = \overline{\mathbf{C}} \backslash J(R)$, the Fatou set, is the set of all $z \in \overline{\mathbf{C}}$ for which the family $R^n(z)$ is equicontinuous, in the spherical metric on some neighborhood of each point of F.

Some important properties of $J(R)$ are listed below:

(a) $J \neq \varnothing$ and J is closed;

(b) J is invariant with respect to R, i.e., $R(J) = J = R^{-1}(J)$;

(c) $J(R) = J(R^m)$, $m = 2, 3, 4, \ldots$;

(d) If J has interior points then $J = \overline{\mathbf{C}}$;

(e) $J(R)$ is compact and nondenumerable. In general, its Hausdorff-Besicovitch dimension is nonintegral, whereupon $J(R)$ is a fractal, as defined by Mandelbrot [20].

Let p be an attractive fixed point of $R(z)$. The *attractive basin* (stable set) $W(p)$ of p is defined as the set

$$W(p) = \left\{z \in \overline{\mathbf{C}} \middle| R^n(z) \to p \text{ as } n \to \infty\right\}.$$

The *immediate attractive basin* $A(p)$ of p is the maximal domain containing p on which the sequence of iterates $\{R^n\}$ is normal. We now have the following important property: the boundary of $W(p)$ is $J(R)$. It follows that if $R(z)$ has several distinct attractive points, then their basins of attraction share the same boundary, the Julia set of $R(z)$.

For iteration schemes involving rational maps, e.g., Newton's method for polynomials, it follows that the forward orbits of all points on $J(R)$ never converge to the roots of the polynomial.

3. Attractive Basins and Julia Sets for Schröder Functions: A Case Study for the Polynomials $g_n(z) = z^n - 1$. In this section we examine, by means of computer-generated plots, the attractive basins and Julia sets of the Schröder functions $S_m(z)$,

$m = 2, 3$, and 4, constructed to converge to the nth roots of unity. The pictures were computed as follows. A square grid of 80,000 points, composed of 400 columns and 200 rows corresponding to the pixels of a computer video display (the 2:1 ratio corresponds to the height-width ratio of each pixel), would represent a region of the complex plane, typically the square $\mathbf{R} \times \mathbf{R} = [-1, 1] \times [-1, 1]$. Given a polynomial $g_n(z) = z^n - 1$ and a map $S_m(z)$, each grid point would be used as a starting value z_0 of the sequence $z_{k+1} = S_m(z_k)$. After each step, the Euclidean distances between the iterate z_k and each nth root of unity were computed. As soon as any of these distances became less than or equal to 0.1, it was assumed that the sequence would converge to that particular root. The pixel corresponding to the original grid point z_0 would then be assigned a particular color, according to the root it converged to. If the procedure did not converge within a typical maximum of 100 iterations, the routine would automatically skip to the next grid point. In most cases, a geometrical symmetry was exploited to reduce calculations to one-half or one-quarter of the grid. In this way, the attractive basin $W(z_i^*)$ for each root of unity z_i^* would be assigned a characteristic color.

The microcomputer-generated plots of these basins in the region $[-1, 1] \times [1, 1]$ are presented in Figures 1, 2 and 3 as families of $S_m(z)$ mappings, $m = 2, 3, 4$, associated with the polynomials $g_n(z) = z^n - 1$. For a given polynomial $g_n(z)$, the basin maps possess the same geometrical symmetries. However, their "complexity" increases with the order m of the $S_m(z)$ maps. New sets of "petals" appear to be embedded in lower order maps in an infinitely self-similar fashion. In all cases, the Julia sets $J(S_m(z))$ are fractal-like and possess remarkable self-similarity.

The white regions surrounding the origin in some of the figures is not to be interpreted as part of a stable set $W(z^*)$. Since $g'(0) = 0$, $z = 0$ is mapped to the point $z = \infty$. Points near $z = 0$ may first be mapped many orders of magnitude away from it, whereupon a great number of iterations—certainly more than the typical maximum of 100 employed in the text—might be required to bring them back to the z_i^*, if at all. As such, these grid points would remain as part of the black background, which has been plotted as white.

The following analysis of these plots considers individually each iteration procedure $S_m(z)$ as applied to the $g_n(z)$. In all cases, the nth roots of unity are denoted as $z_{i,n}^*$, $i = 1, 2, 3, \ldots, n$, $n = 1, 2, 3, \ldots$.

Case 1. $m = 2$: $S_2(z)$, *Newton's Method*. Figures 1(a), 2(a), and 3(a) show the attractive basins $W(z_{i,n}^*)$ associated with the $g_n(z)$, $n = 2, 3$ and 4, respectively. For $n = 2$, it is well known (the Cayley problem [23]) that $W(-1) = L$, $W(+1) = R$, where $L = \{z \in \bar{\mathbf{C}} \,|\, \mathrm{Re}(z) < 0\}$ and $R = \{z \in \bar{\mathbf{C}} \,|\, \mathrm{Re}(z) > 0\}$. In other words I, the imaginary axis, is the Julia set $J(S_2(z))$. In this particular case, the inverses $S_{2,i}^{-1}(z)$ for which $J(S_2(z))$ is an attractor, are easily computed. In the language of Barnsley and Demko [2], I is the attractor for the *iterated function system* (IFS) $\{\bar{\mathbf{C}}, w_+(z), w_-(z)\}$, where

$$w_+(z) = z + \sqrt{z^2 - 1}\,, \qquad w_-(z) = z - \sqrt{z^2 - 1}\,.$$

The Newton attractive basin plots associated with $n = 3$ have appeared elsewhere [12], [23].

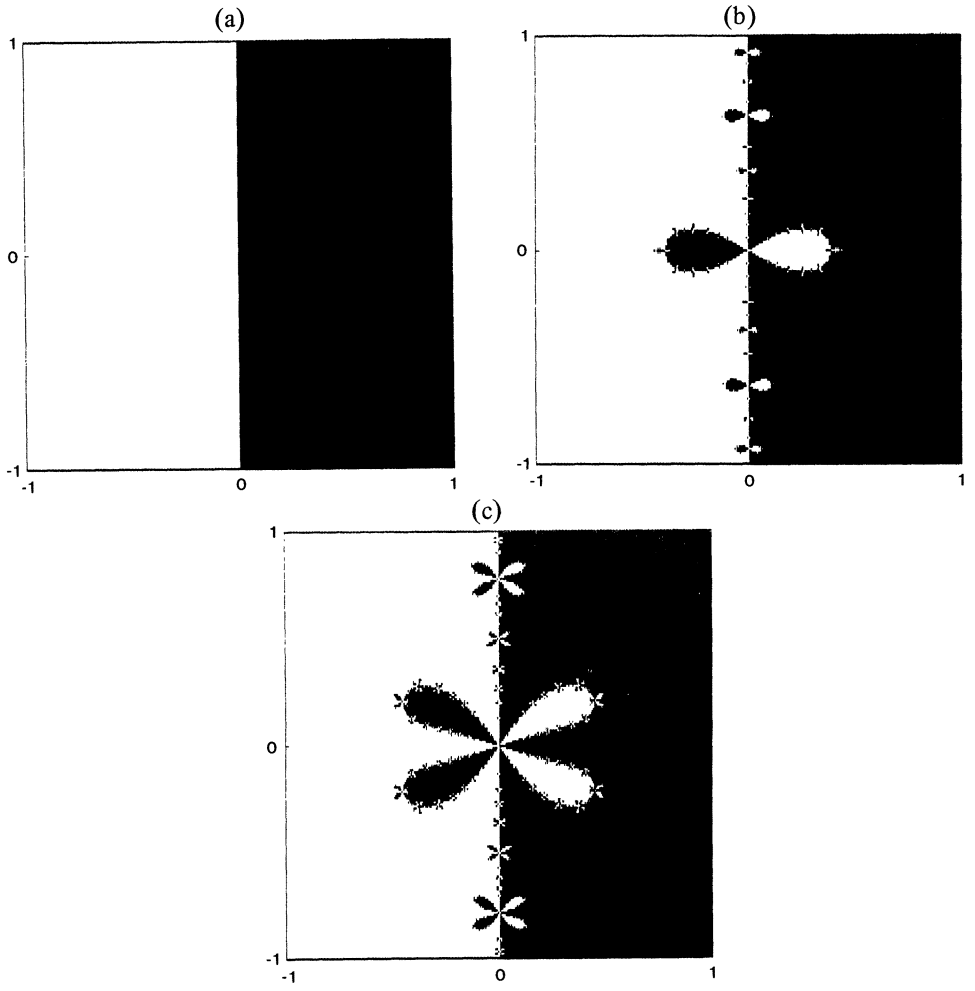

FIGURE 1

Schröder basins of attraction $W(z_i^*)$ for the roots of $g_2(z) = z^2 - 1$ in the complex region $[-1,1] \times [-1,1]$. The black areas comprise the stable set $W(1)$; the white areas comprise the stable set $W(-1)$.

(a) S_2 (Newton) method with quadratic convergence: the Julia set $J(S_2)$, the boundary between $W(1)$ and $W(-1)$, is the imaginary axis.
(b) S_3 method with cubic convergence.
(c) S_4 method with quartic convergence.

Case 2. $m = 3$: *Cubic Convergence.* Manipulation of Eq. (2.7) reveals that the fixed point condition $S_3(z) = z$ implies that either (i) $g_n(z) = z^n - 1 = 0$ or (ii):

$$z^n - \left[\frac{n-1}{3n-1}\right] = 0, \qquad n = 2,3,4,\ldots.$$

An additional n fixed points of $S_3(z)$, which we denote as $\xi_{i,n}$, exist between the roots $z_{i,n}^*$ and $z = 0$. For $n = 2,3,4,\ldots$ all $\xi_{i,n}$ are repulsive fixed points, since

$$S_3'(z)\big|_{z=\xi_{i,n}} = \frac{2(2n-1)}{n-1} > 1, \qquad n = 2,3,4,\ldots.$$

Thus, the ξ_{in} must be on the Julia sets $J(S_3(z))$ for $n \geqslant 2$. This property destroys the Newton "funnels of convergence" exhibited by the immediate stable set $A(z_{in}^*)$ which surround each root z_i^* in Figures 1(a), 2(a) and 3(a), and extend well toward

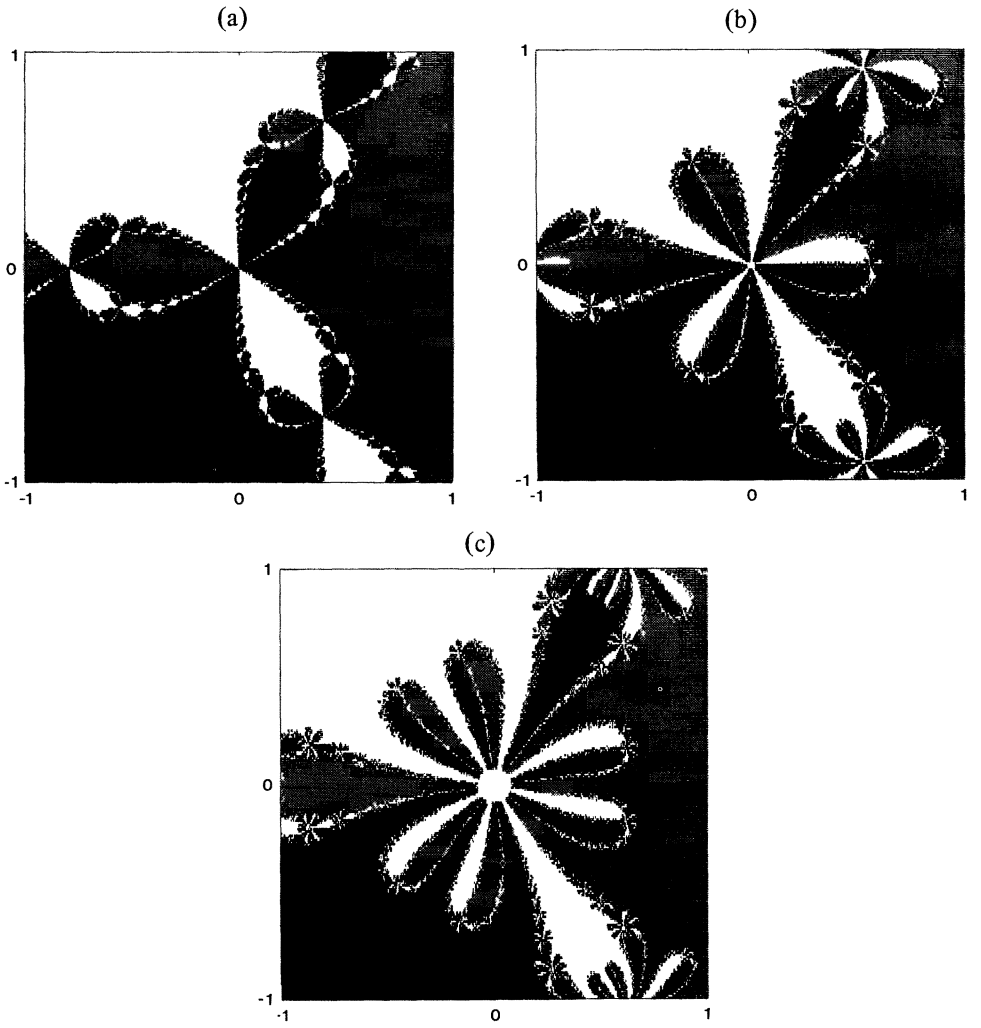

FIGURE 2

Schröder basins of attraction $W(z_i^*)$ for the roots of $g_3(z) = z^3 - 1$ in the complex region $[-1,1] \times [-1,1]$. White regions constitute $W(-\frac{1}{2} + \frac{1}{2}\sqrt{3})$; black regions constitute $W(-\frac{1}{2} - \frac{1}{2}\sqrt{3})$; grey regions constitute $W(1)$.

(a) S_2 (Newton) method.
(b) S_3 method.
(c) S_4 method.

the origin. The attractive basins for $n = 2, 3$, and 4 are presented in Figures 1(b), 2(b) an 3(b), respectively. The appearance of these extra fixed points is a striking example of the caution that is necessary in the selection of initial values of higher-order iteration sequences.

Case 3. $m = 4$: *Quartic Convergence*. The fixed point condition $S_4(z) = z$ implies (i) $z^n - 1 = 0$ or (ii):

$$(z^n - r_n)(z^n - \bar{r}_n) = 0,$$

where

$$r_n = \frac{7n^2 - 9n + 2 + n^2(39n^2 - 54n + 15)^{1/2} i}{22n^2 - 12n + 2}.$$

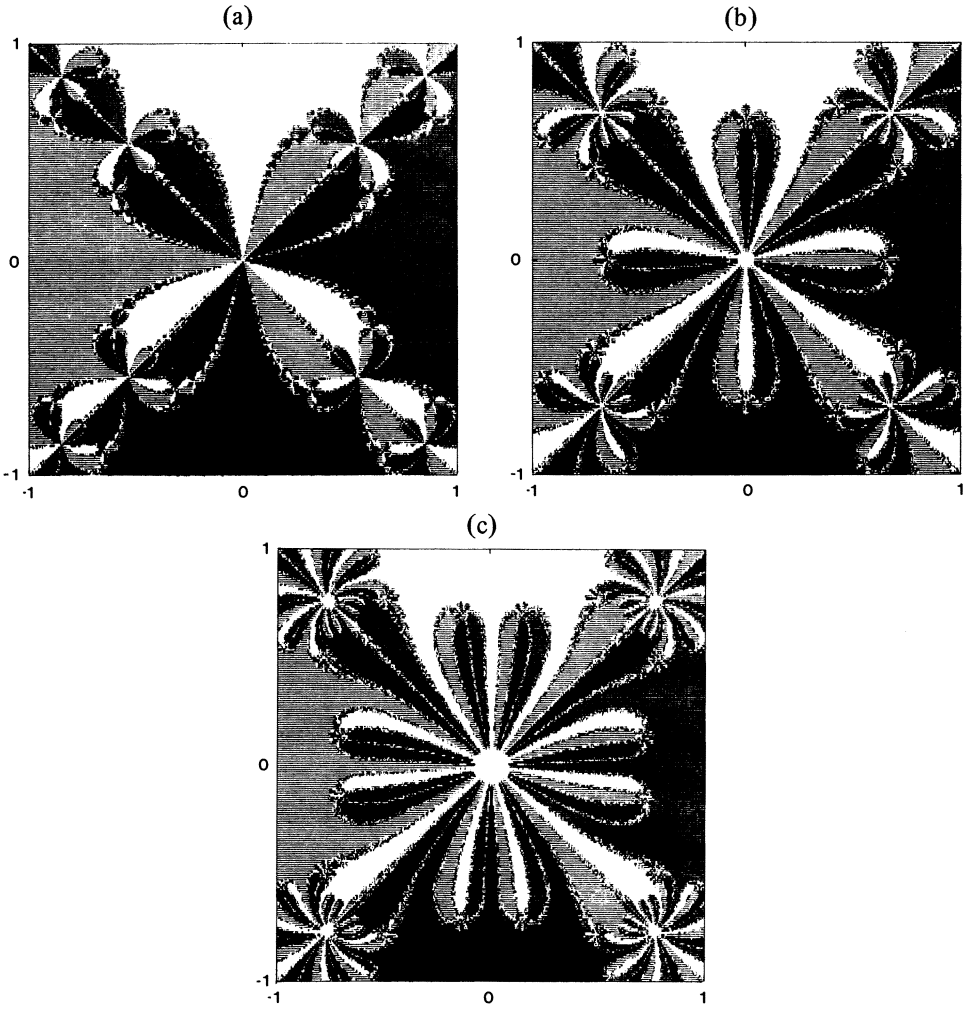

FIGURE 3

Schröder basins of attraction $W(z_i^*)$ for the roots of $g_4(z) = z^4 - 1$ in the complex region $[-1, 1] \times [-1, 1]$. White regions constitute $W(i)$; black regions, $W(-i)$; light grey regions, $W(-1)$; dark grey regions, $W(+1)$.

(a) S_2 (Newton) method.
(b) S_3 method.
(c) S_4 method.

In this case a pair of complex conjugate fixed points μ_{in}, $\bar{\mu}_{in}$ appear in the Newton "funnel of convergence" for each z_i^*. This feature is illustrated in Figures 1(c), 2(c) and 3(c) for $n = 2, 3$ and 4, respectively.

4. The Schröder Iteration Method in Parameter Space. We now focus attention on Schröder iteration methods associated with a particular one-parameter family of cubic polynomials,

$$g_A(z) = z^3 + (A - 1)z - A, \tag{4.1}$$

the zeros of which are $z_1^* = 1$, $z_2^* = -\frac{1}{2} + \frac{1}{2}\sqrt{1 - 4A}$ and $z_3^* = -\frac{1}{2} - \frac{1}{2}\sqrt{1 - 4A}$. In this section, the A-dependence of z_2^* and z_3^* will be understood. We shall now be

working in a parameter space where $A \in \mathbf{C}$. Each point $A = (\mathrm{Re}\,A, \mathrm{Im}\,A)$ represents a dynamical system with its own fixed points, possible attractive cycles and Julia sets. The special case $A = 1$ has already been covered in Section 3 for $n = 3$.

This study represents an extension of the work of Curry et al. [8] in which the Newton-S_2 method associated with the $g_A(z)$ was analyzed. They discovered regions in the A parameter space where attractive periodic cycles exist in addition to the attractive fixed points associated with the zeros of $g_A(z)$. This feature is also observed for higher-order Schröder functions; in addition, extra fixed points corresponding to the roots of Eq. (2.8), shown to be repulsive for $A = 1$, may become attractive in regions of the A-plane.

To detect the existence of attractive cycles which could interfere with the Schröder search for the z_i^*, we observe the orbits of the critical points of the $S_m(z)$ functions. *Critical values* of a function $f(z)$ are defined as those values $v \in \mathbf{C}$ for which $f(z) = v$ has a multiple root. The multiple root $z = c$ is called the *critical point* of $f(z)$. This is equivalent to the statement $f'(c) = 0$. The underlying reason for studying these special orbits rests in the following theorem of Fatou [13]:

THEOREM 4.1. *If $R(z)$ is a rational function having an attractive periodic cycle, then at least one critical point will converge to it.*

Among the critical points of the Schröder functions $S_m(z)$, determined by the condition $S_m'(z) = 0$, are the zeros z_i^* which are also attractive fixed points of the $S_m(z)$. These points are obviously not free to converge to any other attractive cycles. Other roots, which we shall call the *free critical points* c_i, are available, however. The free critical points for the first three $S_m(z)$ functions associated with $g_A(z)$ are given below:

$$\text{(4.2a)} \qquad \text{(i)} \quad S_2(z)\colon\ c_1 = 0,$$

$$\text{(4.2b)} \qquad \text{(ii)} \quad S_3(z)\colon\ c_{1,2} = \pm\left[\frac{A-1}{15}\right]^{1/2},$$

$$\text{(4.2c)} \qquad \text{(iii)} \quad S_4(z)\colon\ c_{1,2} = \pm\left[\frac{A-1}{6}\right]^{1/2}, \qquad c_3 = 0.$$

The dynamics of each Schröder map $S_m(z)$ in complex parameter space was studied in much the same way as described in Section 3. A region of the complex A-plane was again represented by a grid of 400×200 points, corresponding to the pixels of a computer video terminal. For each point $A = (\mathrm{Re}\,A, \mathrm{Im}\,A)$, a free critical point c_i was computed and used as a starting value z_0 for the iteration sequence $z_{k+1} = S_m(z_k)$. After each iteration, the distances between the iterate z_k and the zeros z_i^* of $g_A(z)$ were computed. If any of the distances were less than 0.0001, it was assumed that the sequence was converging to the corresponding root z_i^* and the grid point in A-space was colored accordingly. If, after 200 iterations, no such convergence was observed, the grid point was left black. The resulting black areas represented regions in parameter space for which additional attractive cycles existed.

More detailed investigations of A-values associated with k-cycles and period doubling bifurcations, to be described later in this section, were performed in double-precision (32 significant digit) accuracy on the university CYBER 180/855 mainframe computer.

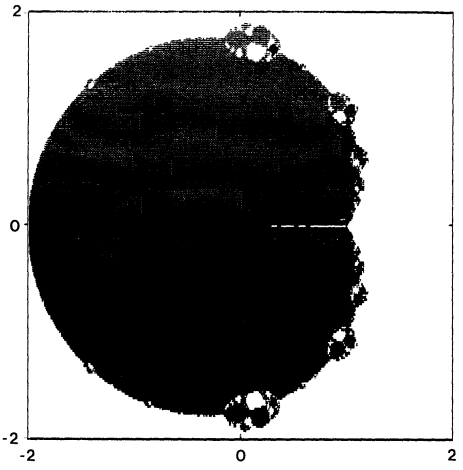

FIGURE 4

S_2 (Newton) iteration scheme for the one-parameter family of cubic polynomials $g_A(z)$ of Eq. (4.1): Regions in the complex parameter space $A \in [-2,2] \times [-2,2]$ for which the forward orbits of the free critical point $c_1 = 0$ converge to $z^* = 1$ (white), the other two roots z_2^* and z_3^* (grey), or none of these roots (black).

Case 1. $m = 2$: *Newton's Method.* As mentioned, this case has been studied [8] and computer plots are presented here for comparison and reference. Figure 4 represents the region of the complex A-plane $[-2,2] \times [-2,2]$. White regions represent values of A for which the sole critical point $c_1 = 0$ is attracted to the root $z_1^* = 1$, gray regions correspond to attraction to either of the roots $z_{2,3}^* = -\frac{1}{2} \pm \frac{1}{2}\sqrt{1 - 4A}$. The small black areas situated at $A \cong (0.31, \pm 1.64)$ and $(1.01, \pm 0.98)$ represent sets of parameter values for which the critical point does *not* converge to a zero of $g_A(z)$. Since no other fixed points exist, these orbits are asymptotic k-cycles, $k \geqslant 2$. When magnified, these regions have the same general shape as the remarkable Mandelbrot bifurcation sets for quadratic maps $R(z) = z^2 - \lambda$. A magnification of the set situated at $(0.31, 1.64)$ is presented in [8]. The existence of stable periodic cycles as well as regions of period-doubling bifurcations in this set has also been shown.

Within the resolution of the plot in Figure 4, four other sets are detected on the real axis at $A \cong 0.26$, 0.36, 0.5 and 0.65. When magnified, the characteristic Mandelbrot shapes appear, as shown in Figure 5 for the region $[0.35, 0.37] \times [-0.01, 0.01]$.

Case 2: $S_3(z)$ *Iteration.* Figure 6 represents regions in parameter space $A \in [-5,5] \times [-5,5]$, for which the critical point c_1 in Eq. (4.2b) is attracted to either $z_1^* = 1$ (white regions), $z_{2,3}^* = -\frac{1}{2} \pm \frac{1}{2}\sqrt{1 - 4A}$ (gray) or neither (black). The corresponding parameter space map for the critical point $c_2 = -c_1$ is obtained by a reflection of Figure 6 about the real A axis. Figure 7 is an enlargement of the region $[1.89, 1.95] \times [-0.03, 0.03]$, but reflected about the real axis. The upper half (including real axis) of this Mandelbrot-like set corresponds to A values for which c_1 does not converge to the z_i^*, the lower half corresponds to the critical point c_2. Unlike in the Newton iteration method, there are two possibilities for the orbits of the c_i to be

trapped away from the roots z_i^*:

(i) convergence to a k-cycle as in Case 1,

(ii) convergence to additional attractive fixed points ξ_i which satisfy Eq. (2.8) for $g(z) = g_A(z)$, i.e., the equation

$$12z^4 + 9(A-1)z^2 - 3Az + (A-1)^2 = 0.$$

In Section 2, these three fixed points were repulsive for the special case $A = 1$.

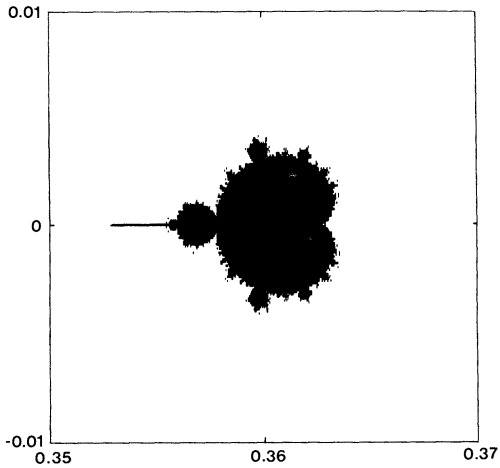

FIGURE 5

A magnification of the black region lying on the real axis of Figure 4 at $A \cong (0.36, 0)$. For values of A lying in this Mandelbrot-like set, there exist attractive k-cycles for the S_2-Newton iteration scheme, distinct from the roots z_i^* of $g_A(z)$.

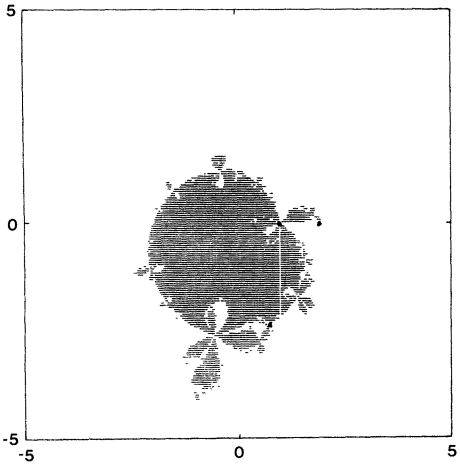

FIGURE 6

S_3 iteration scheme for the one-parameter family of cubic polynomials $g_A(z)$ of Eq. (4.1): Regions in the complex parameter space $A \in [-5,5] \times [-5,5]$ for which the free critical point $c_1 = \sqrt{(A-1)/15}$ in Eq. (4.2b) converges to $z^* = 1$ (white), the roots z_2^* or z_3^* (grey), or none of these roots (black). The corresponding regions for the critical point $c_2 = -c_1$ are obtained by reflecting this figure about the real-A axis. The white vertical strip lies on the line $\mathrm{Re}(A) = 1$.

A more detailed examination of the orbits of critical points reveals that the interior of the largest cardioid of the Mandelbrot set in Figure 7, which intersects the real A axis on the approximate interval [1.921, 1.945], corresponds to A-values for which property (ii) holds. This set does not include the smaller "buds" which grow on its boundary. The cardioid region to its left, intersecting the real A axis on the approximate interval [1.9115, 1.921], corresponds to asymptotic 2-cycles. Real values of A slightly less than 1.9115 have been observed to produce asymptotic 4-cycles.

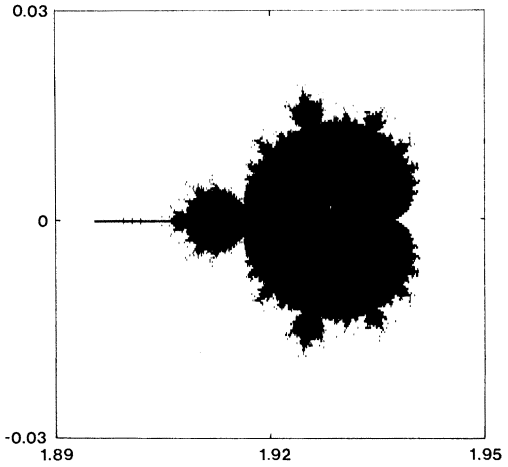

FIGURE 7

A magnification of the parameter space region $[1.89, 1.95] \times [-0.03, 0.03]$ of Figure 6, revealing a Mandelbrot set for the S_3 iteration method.

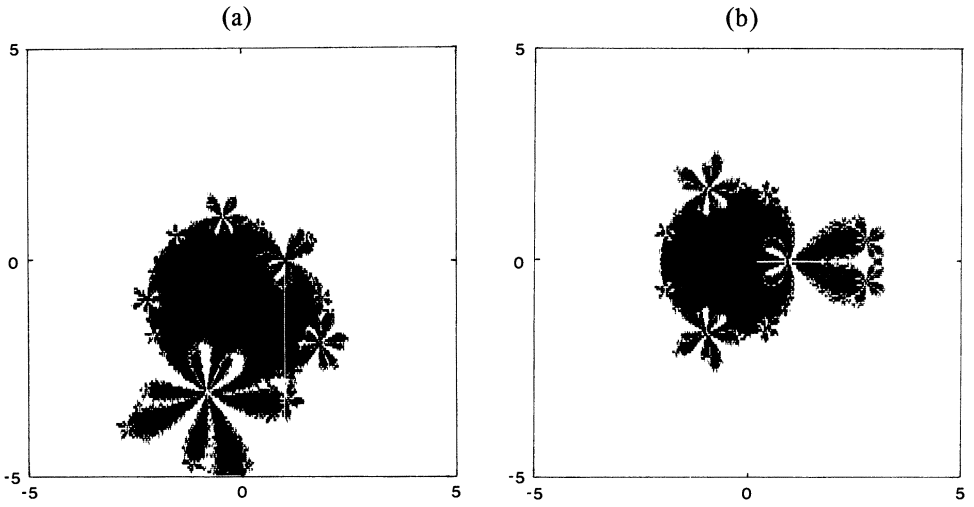

FIGURE 8

S_4 iteration scheme for the one-parameter family of cubic polynomials $g_A(z)$ of Eq. (4.1): Regions in the complex parameter space $A \in [-5, 5] \times [-5, 5]$ for which the free critical points (a) $c_1 = \sqrt{(A-1)/6}$ and (b) $c_3 = 0$ converge to the roots $z^* = 1$ (white), z_2^* or z_3^* (grey), or none of these roots (black). The regions corresponding to $c_2 = -c_1$ may be obtained by reflecting (a) about the Re(A) axis.

Case 3: $S_4(z)$ *Iteration.* Figure 8(a) represents regions in parameter space $A \in [-5, 5] \times [-5, 5]$ for which the critical point c_1 in Eq. (4.3c) is attracted to either $z^* = 1$ (white regions), $z^* = -\frac{1}{2} \pm \frac{1}{2}\sqrt{1 - 4A}$ (grey) or neither (black). The corresponding parameter space map for the critical point $c_2 = -c_1$ is again obtained by a reflection of Figure 8(a) about the real A axis. Figure 8(b) is the parameter space map for the third critical point $c_3 = 0$. Figure 9 is an enlargement of the region $[3.07, 3.17] \times [-0.05, 0.05]$ in Figure 8(b) showing a Mandelbrot-like set associated with $c_3 = 0$. As in the previous case, there exist two possibilities for the orbits of the c_l associated with the Mandelbrot set A-values: (i) convergence to a k-cycle or (ii) convergence to additional attractive fixed points ξ_l which, in this case, are solutions of Eq. (2.8) for $g(z) = g_A(z)$. As before, the large cardioid which intersects the real A axis along the interval $[3.119, 3.1596]$ corresponds to convergence of the critical point c_3 to an extra fixed point ξ_i. The adjacent region associated with the real interval $[3.101, 3.119]$ corresponds to convergence of c_3 to asymptotic 2-cycles. At $A = 3.097$ a transition from real 4-cycles to real 8-cycles is observed numerically.

In all of the above-cited cases of Mandelbrot-like sets, the "pinch points" represent points of pitchfork bifurcation where 2^n-cycles give birth to 2^{n+1}-cycles. This succession of changes follows the now classical pattern, studied by Myrberg [22], Feigenbaum [14], Douady and Hubbard [10] and others. The appearance of these Mandelbrot-like sets suggests that for each m, $S_m(z, A)$ constitutes a Mandelbrot-like family of polynomial-like maps, to use the terminology of Douady and Hubbard [11], being conjugate to the quadratic map $z^2 - \lambda(A)$ in a vicinity of its Julia set. This conjugacy is discussed in detail in [11].

These observations lead us to define, for convenience, the Mandelbrot set $M_m(A)$ associated with the Schröder function $S_m(z)$ for the cubic polynomials $g_A(z)$ as the set $M_m(A) = \{A \in \mathbf{C} | \text{there exist attractive } k\text{-cycles}, k = 1, 2, 3, \ldots, \text{ for } S_m(z) \text{ other than the roots } z_i^* \text{ of } g_A(z) = 0\}$.

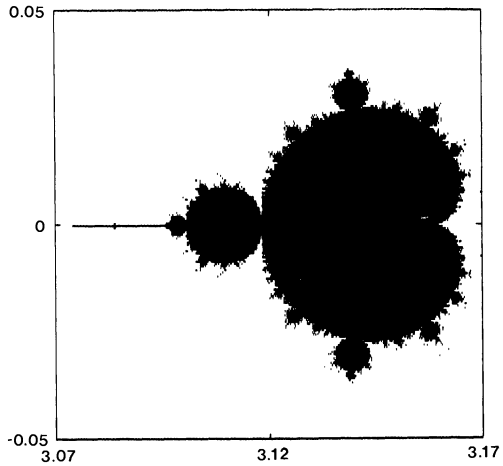

FIGURE 9

A magnification of the complex parameter space region $A \in [3.07, 3.17] \times [-0.05, 0.05]$ of Figure 8(b), revealing a Mandelbrot set for the S_4 iteration method.

5. Julia Sets and Attractive Basins Associated with Pathological Attractive Cycles. We now examine the effects of the Mandelbrot regions $M_m(A)$ in parameter space, discovered in Section 4, on the attractive basin-Julia set maps in complex coordinate space. For $A \in M_m(A)$, the sequence of iterates $S_m^n(z)$, $n = 1, 2, 3, \ldots$ produce attractive k-cycles other than the roots of $g_A(z) = 0$. Attractive basins for such pathological cycles would then presumably appear in the Julia set maps.

Attractive basin maps corresponding to critical values $A \in M_m(A)$ and nearby noncritical values for the Newton-S_2 and S_3 functions, as applied to the $g_A(z)$ cubic polynomials, are presented below. These maps were plotted using the procedure outlined in Section 2.

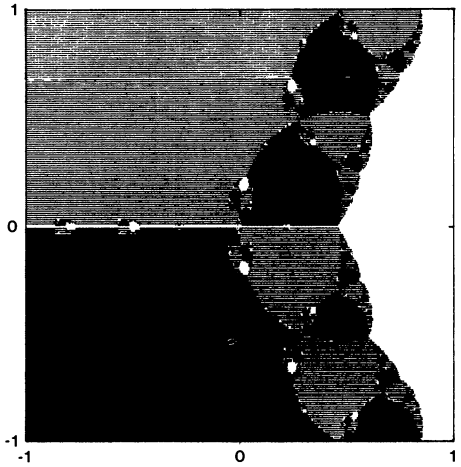

FIGURE 10(a)

Basins of attraction for the roots of $g_A(z)$ for the S_2-Newton method, $A = 0.37$. White regions constitute $W(1)$, the shaded areas constitute $W(z_2^*)$ and $W(z_3^*)$. The Re(z) axis is a part of $W(1)$.

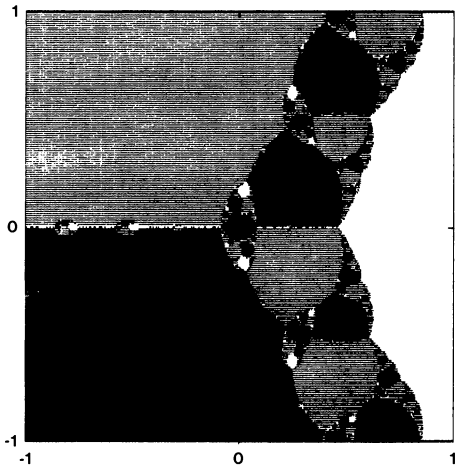

FIGURE 10(b)

Basins of attraction for the roots of $g_A(z)$ for the S_2-Newton method, $A = 0.36$, shaded as in Figure 10(a). The black areas correspond to basins of attraction for an additional attractive two-cycle $p_1 = -0.5628255$, $p_2 = 0.01103592$.

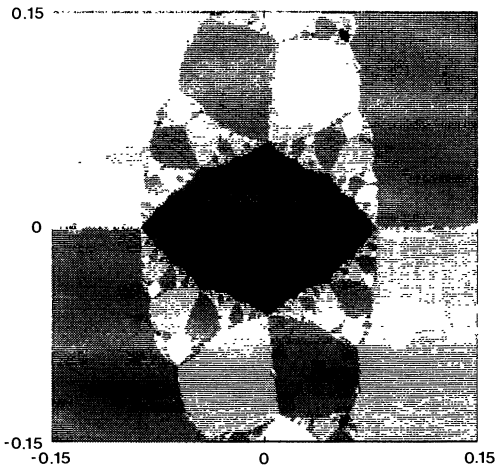

FIGURE 10(c)

A magnification of the region $[-0.15, 0.15] \times [-0.15, 0.15]$ in Figure 10(b), containing one of the attractive basins for the two-cycle.

Newton-S_2 Method. Figures 10(a) and 10(b) show basin maps for the complex region $[-1, 1] \times [-1, 1]$ corresponding to $A = 0.37$ and $A = 0.36$, respectively. A look at Figure 5 reveals that for $A = 0.37$ no attractive k-cycles other than the roots z_i^* exist. For $A = 0.36$, a remarkable change occurs in this map, even though the gross features of the Julia set remain intact. Prominent black regions have appeared at $z = 0, 0.27 \pm 0.49i$ and $0.47 \pm i$. These regions constitute part of the stable set W for the attractive two-cycle $p_1 = -0.5628255$, $p_2 = 0.0110359$. They are also noticeable on a set of "ladybug"-like regions centered on the real axis at roughly $A \cong -0.8$, -0.5 and -0.3. These "ladybugs" have been observed as far out as

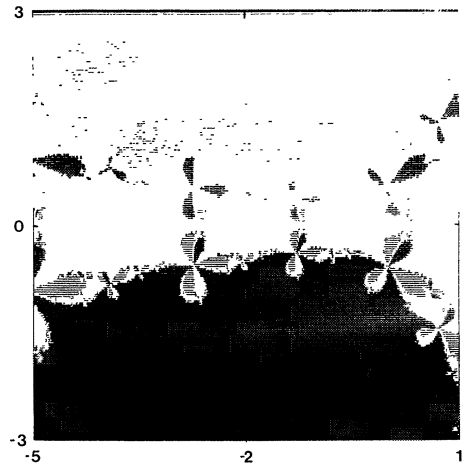

FIGURE 11(a)

Basins of attraction for the roots of $g_A(z)$ for the S_3 iteration method, $A = 1.96$. White regions constitute $W(1)$, the shaded areas constitute $W(z_2^*)$ and $W(z_3^*)$. The Re(z) axis is a part of $W(1)$.

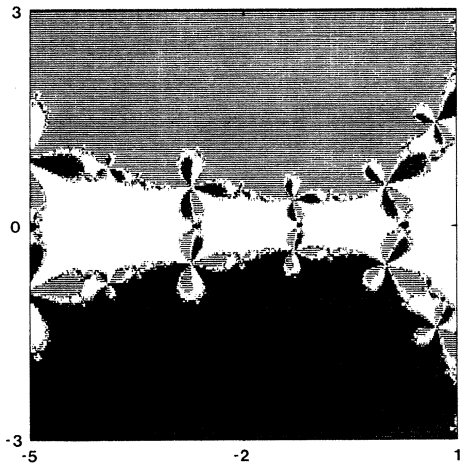

FIGURE 11(b)

Basins of attraction for the roots of $g_A(z)$ for the S_3 iteration method, $A = 1.93$, shaded as in Figure 11(a). The black areas, most noticeably situated on portions of the Re(z) axis where they appear to "sew" attractive basins from the upper and lower halves, correspond to basins of attraction to the extraneous root $\xi = 0.237564$.

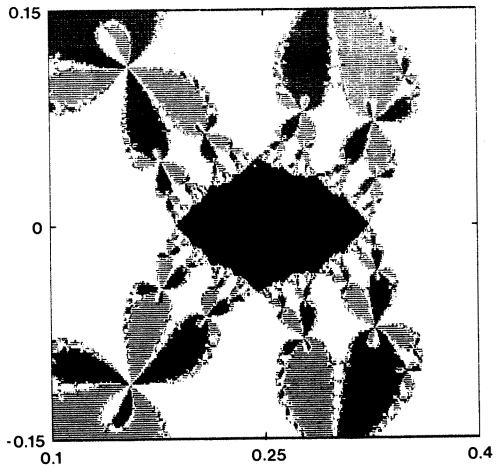

FIGURE 11(c)

A magnification of the region $[0.1, 0.4] \times [-0.15, 0.15]$ in Figure 11(b), containing one of the attractive basins for the extraneous root ξ.

$z = -50$ and are presumed to extend outward to $z \to \infty$. An enlargement of the basin containing the points $z = 0$ and p_2 is presented in Figure 10(c). The multiplier of this two-cycle is $[R^2(p_i)]' \cong 0.371$.

Schröder S_3 Method. Figures 11(a) and 11(b) present basin maps for the complex region $[-5, 1] \times [-3, 3]$ corresponding to $A = 1.96$ (noncritical) and $A = 1.93$ (one extra fixed point $\xi = 0.237564\ldots$ with multiplier $[S_3(\xi)]' \cong 0.655$). For $A = 1.96$, we observe that the stable set of $z = 1$ extends along the negative real axis, passing through narrow "straits". These "straits" have been observed at large negative real

values and, as in the Newton case, are presumed to extend outward as $z \to \infty$. At $A = 1.93$, an actual "sewing" of complex-conjugate basins has taken place. The areas of patching correspond to points which belong to the stable set $W(\xi)$. In Figure 11(b), these areas are located at roughly $A \cong -5.0, -2.68, -1.22$ and 0.24. The basin at 0.24 corresponds to the immediate attractive set of ξ. Figure 11(c), an enlargement of the region containing this basin, reveals the remarkable self-similarity and complexity of the fractal Julia set boundary.

Acknowledgments. The author wishes to thank Professor M. F. Barnsley for stimulating and informative discussions as well as for general advice during the course of this work. The support of a Natural Sciences and Engineering Research Council of Canada Postdoctoral Fellowship for 1984 and 1985 is gratefully acknowledged. Preliminary calculations were performed on a Burroughs B22 minicomputer. All pictures presented in this article were computed on the author's Sanyo MBC-555-2 microcomputer and printed on an Epson FX-80 dot-matrix printer.

School of Mathematics
Georgia Institute of Technology
Atlanta, Georgia 30332

1. L. AHLFORS, *Complex Analysis*, 3rd ed., McGraw-Hill, New York, 1979, pp. 219–227.

2. M. F. BARNSLEY & S. DEMKO, "Iterated function systems and the global construction of fractals", *Proc. Roy. Soc. London Ser. A*, v. 399, 1985, pp. 243–275.

3. M. F. BARNSLEY, J. S. GERONIMO & A. N. HARRINGTON, "Condensed Julia sets, with an application to a fractal lattice hamiltonian," *Trans. Amer. Math. Soc.*, v. 288, 1985, pp. 537–561.

4. M. F. BARNSLEY, T. MORLEY & E. R. VRSCAY, "Iterated networks and the spectra of renormalizable electromechanical networks," *J. Statist. Phys.*, v. 40, 1985, pp. 39–67.

5. P. BLANCHARD, "Complex analytic dynamics on the Riemann sphere," *Bull. Amer. Math. Soc.*, v. 11, 1984, pp. 85–141.

6. H. BROLIN, "Invariant sets under iteration of rational functions," *Ark. Mat.*, v. 6, 1966, pp. 103–144.

7. R. B. BURCKEL, *An Introduction to Classical Complex Analysis*, Academic Press, New York, 1979.

8. J. H. CURRY, L. GARNETT & D. SULLIVAN, "On the iteration of a rational function: computer experiments with Newton's method," *Comm. Math. Phys.*, v. 91, 1983, pp. 267–277.

9. E. DOMANY, S. ALEXANDER, D. BENSIMON & L. P. KADANOFF, "Solutions to the Schrödinger equation on some fractal lattices," *Phys. Rev. B*, v. 28, 1984, p. 3110–3123.

10. A. DOUADY & J. HUBBARD, "Itération des polynômes quadratiques complexes," *C. R. Acad. Sci. Paris Ser. I. Math.*, v. 294, 1982, pp. 123–126.

11. A. DOUADY & J. HUBBARD, "On the dynamics of polynomial-like mappings," 1984. (Preprint.)

12. J. P. ECKMANN, "Savez-vous résoudre $z^3 - 1$?" *La Recherche*, v. 14, 1983, pp. 260–262.

13. P. FATOU, "Sur les équations fonctionelles," *Bull. Soc. Math. France.*, v. 47, 1919, pp. 161–271; v. 48, 1920, pp. 33–94, 208–314.

14. M. FEIGENBAUM, "Quantitative universality for a class of nonlinear transformations," *J. Statist. Phys.*, v. 19, 1978, pp. 25–52.

15. J. GUCKENHEIMER, *Endomorphisms of the Riemann Sphere*, Proc. Sympos. Pure Math., vol. 14, Amer. Math. Soc., Providence, R. I., 1970, pp. 95–123.

16. P. HENRICI, *Applied and Computational Complex Analysis*, vol. 1, Wiley, New York, 1974.

17. J. L. HOWLAND & R. VAILLANCOURT, "Attractive cycles in the iteration of meromorphic functions," 1984. (Preprint.)

18. A. S. HOUSEHOLDER, "Schröder and Trudi: A historical excursion," *SIAM Rev.*, v. 16, 1974, pp. 344–348.

19. G. JULIA, "Mémoire sur l'itération des fonctions rationelles," *J. Math. Pures Appl.*, v. 4, 1918, pp. 47–245.

20. B. MANDELBROT, "Fractal aspects of $z \to \lambda z(1 - z)$ for complex λ and z," *Ann. New York Acad. Sci.*, v. 357, 1980, pp. 249–259. *The Fractal Geometry of Nature*, Freeman, New York, 1983.

21. R. MAÑÉ, P. SAD & D. SULLIVAN, "On the dynamics of rational maps," 1982. (Preprint.)

22. P. MYRBERG, "Iteration der reellen Polynome zweiten Grades," *Ann. Acad. Sci. Fenn.*, v. A256, 1958; "Iteration von Quadratwurzeloperationen," *ibid.*, v. A259, 1958; "Iteration der reellen Polynome zweiten Grades. II," *ibid.*, v. A268, 1959: "Inversion der Iteration für rationale Funktionen," *ibid.*, v. A292, 1960; "Sur l'itération des polynomes réels quadratiques," *J. Math. Pures Appl.*, v. 41, 1962, pp. 339–351; "Iteration der reellen Polynome zweiten Grades. III," *Ann. Acad. Sci. Fenn.*, v. A336, 1964; "Iteration der Binome beliebigen Grades," *ibid.*, v. A348, 1964.

23. H. O. PEITGEN, D. SAUPE & F. V. HAESELER, "Cayley's problem and Julia sets," *Math. Intelligencer*, v. 6, 1984, pp. 11–20.

24. E. SCHRÖDER, "Ueber unendlich viele Algorithmen zur Auflösung der Gleichungen," *Math. Ann.*, v. 2, 1870, pp. 317–365.

25. W. F. SMYTH, "The construction of rational iterating functions," *Math. Comp.* v. 32, 1978, pp. 811–827.

26. D. SULLIVAN, "Itération des fonctions analytiques complexes," *C. R. Acad. Sci. Paris. Ser. I Math.*, v. 294, 1982, pp. 301–303.

27. W. P. THURSTON, "On the dynamics of iterated rational maps." (Preprint.)